

Modeling of piezoelectric coupling coefficients of soft ferroelectrets for energy harvesting

Omar Ben Dali¹, Sergey Zhukov¹, Romol Chadda¹, Perceval Pondrom¹,
Xiaoqing Zhang², Gerhard Sessler¹, Heinz von Seggern¹, and Mario Kupnik¹

¹Technische Universität Darmstadt, Germany,

²Tongji University, Shanghai, China.

Abstract—Recently, Fluoroethylenpropylene (FEP) tubes have been thermally fused to form ferroelectrets with a parallel-tunnel structure with well-defined air gaps thereby improving their applicability for energy harvesting applications. These structures exhibit mechanical and electric properties, mostly depending on their geometry, which result in structure-specific longitudinal and transversal piezoelectric coupling coefficients (d_{33} and d_{31}). This work presents a finite element model able to describe the mechanical-to-electrical coupling of FEP parallel tunnel structures. The focus of the presented paper, however, lies singularly on the coefficient d_{33} , neglecting the transversal coupling coefficient d_{31} . The coupling coefficient d_{33} is calculated in three main steps. First, the induced charge on the electrode's surface for the unloaded state is determined. Second, the deformation of the structure due to an external force applied in thickness direction is computed. Third, the modified shape is used to determine the electrode's charge variation. The model correctly predicts the experimental values for the Young's moduli in the range of 0.6 MPa to 0.9 MPa, within 10%. The piezoelectric coefficient d_{33} is predicted for two internal charge densities, namely $3 \times 10^{-4} \text{ C/m}^2$ and $5 \times 10^{-4} \text{ C/m}^2$. The respective d_{33} coefficients are 110 and 240 pC/N. This is in excellent agreement with measured values of 120 and 180 pC/N, respectively. The results prove the finite element model to be suitable to calculate the piezoelectric coupling coefficients for different types of geometries.

Index Terms—FEA Modeling, Energy Harvesting, Ferroelectret, Piezoelectret

I. INTRODUCTION

Energy harvesting is defined as the extraction of electrical energy from ambient sources such as temperature, vibration or air currents for low power mobile devices. Although such devices have been investigated and even commercialized, the field is still very active and new and better solutions are required. In fact, sensor networks, which do not require batteries and transmit their data by wireless technologies are increasingly being used for monitoring of widely distributed production and process engineering plants. In this context, energy harvesters are seen as the driving force behind industry 4.0 applications, as a way to supply these devices with energy, where electric power is not readily available.

A recent development in vibration based energy harvesting is the use of devices based on polymer ferroelectrets [1]–[5].

The work has been funded by the Deutsche Forschungsgemeinschaft (DFG) Grants Nr. SE 941/19-1, SE 941/21-1, KU 3498/1-1 and from the Natural Science Foundation of China (NSFC) Grant Nr. 61761136004.

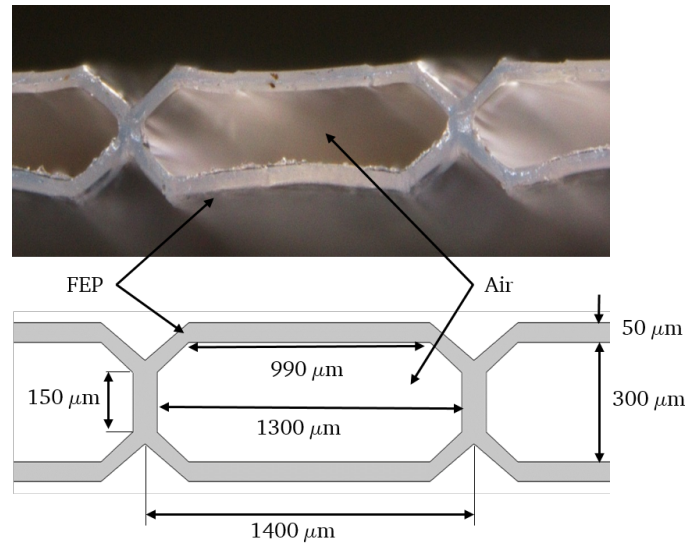


Fig. 1. Comparison of the structure geometry corresponding to one of the measured samples with the geometry simulated. The modeled structure geometry in Comsol Multiphysics features a 50 μm thick FEP layer, which reproduces the manufactured geometry.

These are usually non-polar polymer foams or polymer systems with internally charged cavities [6]. The energy harvester discussed in this paper can be considered as a ferroelectret, which has been produced by deforming a commercial Teflon FEP tube array in a way to artificially possess stadium-like, breakdown-charged air cavities (Fig. 1) referred to as tubular-array-structure [7]. These structures feature an additional design freedom and therefore form films with mechanical properties, mostly dependent on the geometry and the stiffness of the structure.

The goal of this paper is to investigate these newly developed polymer structures for their applicability as energy harvester systems. Since the performance of the ferroelectret is influenced by the interplay of electrical and mechanical properties, it is key to analyze the impact of these contributions on the final piezoelectric response. Due to the complicated geometry, an analytical determination of their properties only is possible with certain simplifying assumptions. In order to achieve a better understanding, a finite element analysis (FEA) will be performed.

II. MODELING OF THE FEP-TUBE'S ELECTRO-MECHANICAL BEHAVIOUR

A. Modeling of the electrical behaviour

After preparation of the tubular-array-structure, through deforming Fluoroethylenpropylene (FEP) tubes to a sequence of stadium-like structures, electrodes are applied to both sides of the structure. Thereafter, the charging of the ferroelectret sample is performed by clamping the sample between positive and negative electrodes of a high voltage power supply (Model HCN 35-6 500, FuG Elektronik, Schechen, Germany). The charging process results in creating a surface charge density at the inner air/FEP interfaces, which remains trapped after the applied voltage has been turned off. The trapped charge density σ_{int} (internal charge density) can be calculated using (1) when the charging voltage V is greater than the threshold voltage V_B and smaller than $2V_B$ [8], [9], i.e.

$$\sigma_{\text{int}}(V) = \varepsilon_0 \left[\frac{\varepsilon_p}{2d_p} V - \left(\varepsilon_g + \frac{\varepsilon_g d_g}{2d_p} \right) E_B \right], \quad (1)$$

where V is the poling voltage, E_B is the breakdown field in the airgap between the two FEP layers, d_p and d_g are FEP layers and air gap layer thicknesses respectively, and ε_p and ε_g are the relative dielectric permittivities, respectively. This internal charge density is the remaining charge density after the applied voltage has been turned off and the sample is short-circuited. If the poling voltage V reaches or exceeds $2V_B$, then we can assume that the maximum possible remanent internal charge density $\sigma_{\text{int}}^{\text{max}}$ is attained and can be calculated as [10]

$$\sigma_{\text{int}}^{\text{max}}(V) = E_B \left(\varepsilon_0 \varepsilon_g + \varepsilon_0 \varepsilon_g \frac{d_g}{2d_p} \right). \quad (2)$$

The theoretical model (1) applies for a device with two parallel solid blocking layers separated by an air gap. Therefore, it only is used to estimate the required electrical voltage to reach the maximum remanent internal charge density $\sigma_{\text{int}}^{\text{max}}$. The calculated value is from here on used as a benchmark for the following simulations.

The charge density σ_{int} induces a surface charge density σ_0 in the electrodes (Fig. 2) which can be determined using Gauss' law and Kirchhoff's second law under short-circuit conditions. It yields [11]

$$\sigma_0 = \frac{d_g \varepsilon_p}{\varepsilon_p d_g + 2\varepsilon_g d_p} \sigma_{\text{int}}. \quad (3)$$

Following the same reasoning, we define an internal charge density σ_{int} as a boundary condition for our FEA Model. After solving the continuity equation between different media using Gauss's law, we calculate the induced charge in the electrodes. The relevant interface conditions for this case were solved by COMSOL Multiphysics through (4) and (5), i.e.

$$n \cdot (D_g - D_p) = \sigma_{\text{int}}, \quad (4)$$

$$Q = \int_A \sigma_0 \cdot dA. \quad (5)$$

where n is the normal vector, A is the electrode area and Q is the electric charge on the electrode. Since the surface charge can be measured, whereas the internal charge can only be calculated, we used Sawyer-Tower-method [12] to determine the surface charge density σ_0 . The measured value is then compared with the simulated one for a better estimation of the internal charge density σ_{int} .

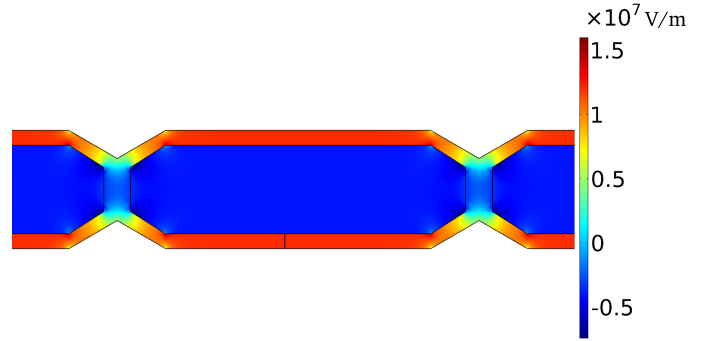


Fig. 2. Simulation result of the electric field for an internal charge density of $\sigma_{\text{int}} = 3 \cdot 10^{-4} \text{ C m}^{-2}$. The induced surface charge density σ_0 is then calculated using a 4th-order integration

If an external mechanical load F is applied to the sample, the air-filled channel thickness d_g will be deformed but the internal charge density σ_{int} remains constant. For this reason, the induced charge on the surface σ_0 will be modified. The variation of $\sigma_0 \pm \Delta\sigma_0$, as a function of the mechanical stress, describes the piezoelectric property of this ferroelectret film, which can be calculated as

$$d_{33} = \frac{\Delta\sigma_0}{\sigma_{\text{mech}}} = \frac{\Delta Q}{F}. \quad (6)$$

Therefore, a proper determination of the deformed geometry due to an exerted force in COMSOL Multiphysics is indispensable for a successful prediction of the piezoelectric coupling coefficient d_{33} .

B. Modeling of the mechanical behaviour

In order to determine the deformation of the tubular-array-structure for a given force, we have chosen a scenario where the tubular-array-structure is fixed at the lower plate, and is pressed by a moving plate in the thickness direction. For simulating the large deformation, the FEP layer has to be defined as a hyperelastic material. Several built-in hyperelastic material models are available in COMSOL Multiphysics. For each of these material models, there are expressions for the total strain energy density function, which require one or more material parameters that have to be extracted from experiments. In this work, only uniaxial tension and compression are considered. Hereby we assume that the isotropic behavior of FEP remains even after heat treatment. Based on the experimental data available, the Neo-Hookean model has been chosen. This definition in COMSOL Multiphysics requires the knowledge of the Lamé parameters, which allow for a parameterization

of the elastic moduli for the FEP layer and can be calculated according to [13] as follows

$$\lambda = \frac{\nu Y}{(1 + \nu)(1 - 2\nu)}, \quad (7)$$

$$\mu = \frac{Y}{2(1 + \nu)}, \quad (8)$$

where λ is the first Lamé parameter, μ the second, ν Poisson's ratio and Y Young's Modulus. The required FEP-layer parameters for the simulated scenario are $Y = 350$ MPa, the density $\rho = 2150$ kg m⁻³, $\nu = 0.48$, $\lambda = 2.8378 \cdot 10^9$ N m⁻² and $\mu = 1.1824 \cdot 10^8$ N m⁻².

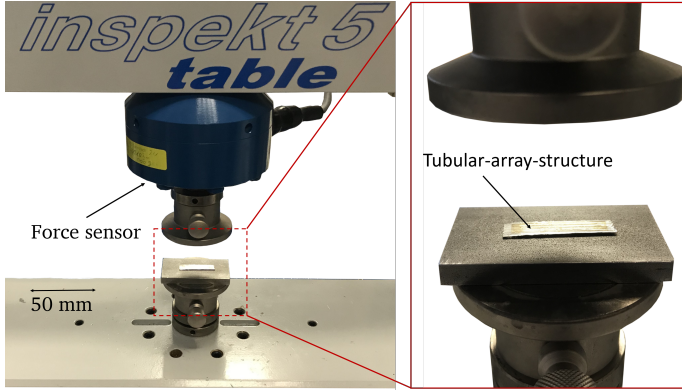


Fig. 3. Experiment setup using the universal testing machine to validate the simulation results. The tubular-array-structure is positioned in the longitudinal direction between the two clamps and is pressed from above. It has been carefully ensured that a strain of 15% is not exceeded.

In order to validate the FEA model for the tubular-array-structures (25mm long tunnels), several arrays with different number of tubes have been fabricated. A greater number of tubes however, raises the probability of defects, resulting in a mechanical non-stability of the merged tubes. Furthermore, the obtained shape of the individual air channels is irregular. In order to overcome this drawback, only tubular-array-structures with three tubes have been investigated. Before the measurement, the shape of the individual channels of each tubular-array-structure was examined, to ensure that they exhibit approximately the same geometry as the modeled one. The measurement is performed using a universal testing machine (Model inspekt Table5, Hegewald & Peschke, Nosse, DE). With the purpose to conduct approximately a quasi-static measurement, we used a velocity of 1 N/s.

C. Prediction of the piezoelectric properties of the tubular-array-structure

For the prediction of the longitudinal piezoelectric d_{33} coefficient in COMSOL, we combine the electrostatics interface and a moving mesh interface with those of a solid mechanics interface. The deformation of the structure, due to an external force is determined in the mechanical model. For each force induced deformation, the electrode charge is calculated for the new resulting geometry. The piezoelectric d_{33} coefficient

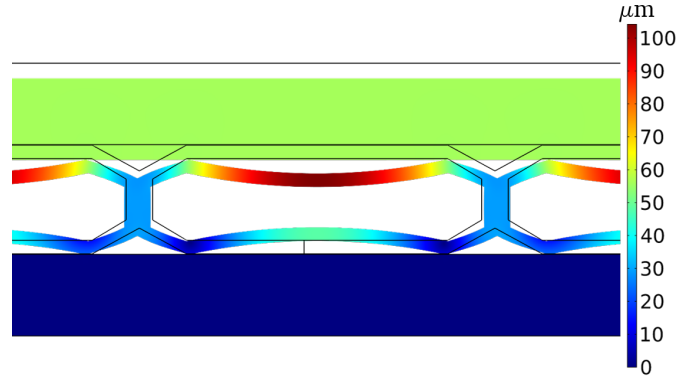


Fig. 4. Deformation of the tubular-array-structure due to the exerted force of the upper plate by moving towards thickness direction for a distance of 60 μm. The color scale refers to the displacements.

is predicted by calculating the change in electrode charge for each geometry variation due to an external load F according to (6).

In order to check the accuracy of the model, samples with the same number of tunnels (three tunnels) have been fabricated and tested under the same boundary conditions. In this paper, the measurement of only three samples is discussed. In order to avoid any interfering charges in the environment, we used a metal shield that acts as a Faraday cage and a triaxial cable to extract the induced charge from the electrodes. Furthermore, a linear guide of the utilized mass causes mechanical pre-stressing when placed onto the sample. Thus, to avoid the effect of pre-stressing, the measurement is performed in two steps. First, a force including the linear guide mass is applied to the sample for 3 mins to achieve a quasi steady state. After removing the force, the induced charge is measured and integrated over 10 s by means of an electrometer to account for mechanical relaxation (Model B2987A, Keysight Technologies, Santa Rosa, California, USA).

III. RESULTS AND DISCUSSION

The measurements of d_{33} coefficients of samples 2 and 3 are in good agreement with the simulation (Fig. 5). By increasing the mechanical stress, the two layers on which the internal charge density is trapped approach each other. This results in a higher surface charge variation. However, the measured d_{33} of sample 1 does not increase with a larger applied stress. This can be explained by the manufacturing tolerances, that results in an inappropriate shape of the tubes during the deformation. Nevertheless, the measured values are in the same range as the simulation.

The piezoelectric coupling coefficient d_{33} of the tubular-array-structure depends not only on the internal charge density σ_{int} but also on the Young's modulus Y as

$$d_{33} \propto \frac{\sigma_{\text{int}}}{Y}. \quad (9)$$

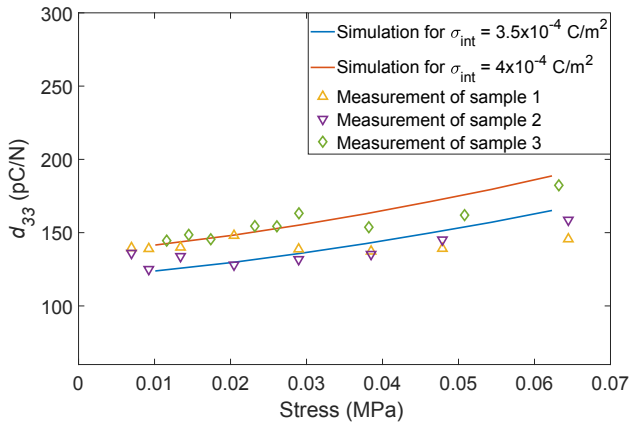


Fig. 5. Experimental and simulation results for the piezoelectric d_{33} coefficient. The symbols correspond to the experimental results, while the solid line represents the simulation.

By increasing the tunnel's length, the surface on which the charge Q is trapped becomes larger. However, the internal charge density σ_{int} remains almost constant as does the the surface charge variation $\Delta\sigma_0$. Furthermore, the Young's modulus Y is not affected by the tunnel's length and therefore the piezoelectric coupling coefficient d_{33} is not affected as well. This is compensated by the increasing number of tunnels. As the number increases, the Young's modulus Y also increases and therefore the piezoelectric coupling coefficient d_{33} decreases (Fig. 6). Applying a mechanical stress onto one tube, results in a transverse stretching on both sides. This is however not the case if several tubes hinder each other on both sides due to frictional and elastic forces. In fact, for the same applied mechanical stress, the tunnels with no restrictions on the sides undergoes a greater deformation, which results in a higher charge variation on the electrodes.

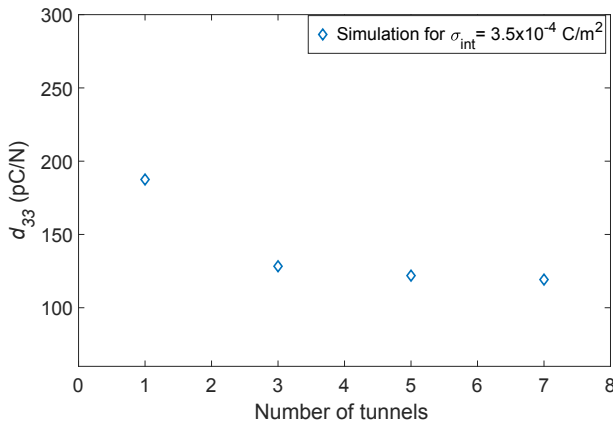


Fig. 6. Influence of increasing the number of tunnels on the piezoelectric d_{33} coefficient. This is calculated for the tubular-array-structure with different tunnel's number, using the same internal charge density $\sigma_{int} = 3.5 \times 10^{-4} \text{ C m}^{-2}$ and the same mechanical stress $\sigma_{mech} = 0.14 \text{ MPa}$.

In this model, Coulomb's law within the structure is not taken into consideration. By increasing the mechanical stress

over 0.07 MPa, The piezoelectric d_{33} decreases. This can't be simulated using the present model described in this work.

IV. CONCLUSION

The presented FEA model provides a possibility for the prediction of the piezoelectric d_{33} coefficient without any assumption to simplify the geometry, as normally done for analytic modeling. This allows a targeted development of new geometries for future ferroelectrets having sufficient stability and optimal coupling coefficients for usage in energy harvesters. This serves also as a basis for further optimization of the tubular-array-structure which can exhibit piezoelectric responses comparable to PZT ceramics with the additional advantages of the light weight, flexibility and wide frequency range.

ACKNOWLEDGMENT

The authors gratefully acknowledge financial support by the Deutsche Forschungsgemeinschaft (DFG) Grants Nr. SE 941/19-1, SE 941/21-1, KU 3498/1-1 and from the Natural Science Foundation of China (NSFC) Grant Nr. 61761136004.

REFERENCES

- [1] S. R. Anton, and K. M. Farinholt, "An evaluation on low-level vibration energy harvesting using piezoelectret foam." *Active and Passive Smart Structures and Integrated Systems*, vol. 8341, p. 83410G, 2012.
- [2] X. Zhang, P. Pondrom, L. Wu, and G. M. Sessler. "Vibration-based energy harvesting with piezoelectrets having high d31 activity." *Applied Physics Letters*, vol. 108, 193903, 2016.
- [3] G. M. Sessler, P. Pondrom, and X. Zhang. "Stacked and folded piezoelectrets for vibration-based energy harvesting." *Phase Transitions*, vol. 89, pp. 667-677, 2016.
- [4] X. Zhang, P. Pondrom, G.M. Sessler and X. Ma, "Ferroelectret nanogenerator with large transverse piezoelectric activity" *Nano energy*, vol. 50, pp. 52-61, 2018.
- [5] Y. Zhang, C. R. Bowen, S. K. Ghosh, D. Mandal, H. Khanbareh, M. Arafa, & C. Wan, Ferroelectret materials and devices for energy harvesting applications. *Nano Energy*, vol. 57, pp. 118-140, 2019.
- [6] G. S. Neugschwandtner, G. S., et al. "Large and broadband piezoelectricity in smart polymer-foam space-charge electrets." *Applied Physics Letters*, vol. 77, pp. 3827-3829, 2000.
- [7] S. Zhukov, D. Eder-Goy, C. Biethan, S. Fedosov, B.-X. Xu, and H. von Seggern, "Tubular fluoropolymer arrays with high piezoelectric response," *Smart Mater. Struct.*, vol. 27, 015010, 2018.
- [8] H. Seggern, S. Zhukov, S. Fedosov, "Importance of geometry and breakdown field on the piezoelectric d 33 coefficient of corona charged ferroelectret sandwiches," *IEEE Transactions on Dielectrics and Electrical Insulation*, vol. 18, pp. 49-56, 2011.
- [9] B.-X. Xu, H. von Seggern, S. Zhukov, and D. Gross, "Continuum modeling of charging process and piezoelectricity of ferroelectrets," *J. Appl. Phys.*, vol. 114, 094103, 2013.
- [10] S. Zhukov, S. Fedosov, H. von Seggern, "Piezoelectrets from sandwiched porous polytetrafluoroethylene (ePTFE) films: Influence of porosity and geometry on charging properties.," *Journal of Physics D: Applied Physics*, vol. 44, 105501, 2011.
- [11] S. Zhukov, D. Eder-Goy, S. Fedosov, B.X. Xu, H. von Seggern, "Analytical prediction of the piezoelectric d 33 response of fluoropolymer arrays with tubular air channels," *Scientific reports*, vol. 8, 4597, 2018.
- [12] E.A. Pecherskaya, "The use of the Sawyer-Tower method and its modifications to measure the electrical parameters of ferroelectric materials." *Measurement Techniques*, pp. 1101-1107, 2007.
- [13] G.Mavko, T. Mukerji, and J. Dvorkin, "The rock physics handbook: Tools for seismic analysis of porous media." Cambridge university press, 2009.